Available online at www.sciencedirect.com
SCIENCE DIRECT
Agricultural and Forest Meteorology 135 (2005) 44–60
AGRICULTURAL AND FOREST METEOROLOGY
www.elsevier.com/locate/agrformet

Feasibility of quantifying ecosystem–atmosphere $C^{18}O^{16}O$ exchange using laser spectroscopy and the flux-gradient method

T.J. Griffis [a,*], X. Lee [b], J.M. Baker [a,c], S.D. Sargent [d], J.Y. King [a,e]

[a] *Department of Soil, Water, and Climate, University of Minnesota-Twin Cities, Borlaug Hall, 1991 Upper Buford Circle, St. Paul, MN 55108, USA*
[b] *School of Forestry and Environmental Studies, Yale University, 370 Prospect Street, New Haven, CT 06511, USA*
[c] *USDA-ARS, St. Paul, MN 55108, USA*
[d] *Campbell Scientific, Inc., 815 West 1800 North, Logan, UT 84321, USA*
[e] *Department of Ecology, Evolution, and Behavior, University of Minnesota-Twin Cities, 100 Ecology Building, 1987 Upper Buford Circle, St. Paul, MN 55108, USA*

Received 12 May 2005; accepted 18 October 2005

Abstract

Stable isotopes of carbon dioxide (CO_2) can be used as natural tracers to better understand carbon cycle processes and exchange pathways between the biosphere and atmosphere. In this study, we used a tunable diode laser (TDL) technique for continuous fast measurement of the stable isotopomers $C^{18}O^{16}O$ and $C^{16}O_2$ and their ratio, δ_a. The TDL system was configured to measure mixing ratios of $[C^{16}O_2]$ and $[C^{18}O^{16}O]$ at wavenumber frequencies of 2308.225 and 2308.416 cm^{-1}, respectively. Two-minute precision (1 standard deviation) was 0.0004, 0.09 μmol mol^{-1}, and 0.26‰ for $[C^{18}O^{16}O]$, $[C^{16}O_2]$ and δ_a, respectively. Comparison of TDL and mass spectrometry flask measurements showed relatively good agreement ($r^2 = 0.94$) with a standard deviation of 0.55‰ for the residual values. Estimates of the isotope signature of ecosystem flux components over a soybean (*Glycine max*) field were examined. These data represent one of the first continuous flux measurements of $C^{18}O^{16}O$. The isotope signature of net ecosystem CO_2 exchange at night ranged from −15 to −7‰ and during the daytime from −40 to −20‰. A simple estimate of canopy-scale photosynthetic discrimination showed significant diurnal variation and averaged 10.5‰ (±8.8‰). The large difference between the isotope signature of respiration and midday canopy photosynthesis represented significant isotopic disequilibrium. Coupled with recent advances in measuring water vapor isotopomers with the TDL technique, a new opportunity is emerging to better understand the dynamics, complex interactions, and discrimination mechanisms controlling land-atmosphere $C^{18}O^{16}O$ exchange.

Keywords: Oxygen isotopes; Carbon dioxide; Water vapor; Tunable diode laser (TDL); Ecosystem discrimination; Flux partitioning

1. Introduction

Quantifying stable isotope ratios of atmospheric carbon dioxide (CO_2) and water vapor and understanding the processes governing their discrimination can help to elucidate complex ecosystem processes involved in the exchange of CO_2 and water vapor between the land and atmosphere (Flanagan and Ehleringer, 1998; Yakir and Sternberg, 2000). Measurements of atmospheric CO_2 isotopes have been used for estimating the isotope signature of ecosystem respiration (Keeling, 1958), photosynthetic discrimination

* Corresponding author. Tel.: +1 612 625 3117.
E-mail address: tgriffis@umn.edu (T.J. Griffis).

0168-1923/$ – see front matter © 2005 Elsevier B.V. All rights reserved.
doi:10.1016/j.agrformet.2005.10.002

(Farquhar et al., 1989; Lloyd et al., 1996), constraining regional sinks and sources of CO_2 (Fung et al., 1997), separating the influence of oceanic from terrestrial CO_2 exchange (Tans et al., 1993) and partitioning micrometeorological estimates of net ecosystem CO_2 exchange (F_N) into gross ecosystem photosynthesis (F_P) and ecosystem respiration (F_R) (Yakir and Wang, 1996; Bowling et al., 2001; Ogée et al., 2003; Zhang, in press).

While the majority of land-atmosphere CO_2 exchange research has used the $^{13}CO_2$ tracer, the $C^{18}O^{16}O$ signal is also needed because it contains unique biophysical information that can be used to help understand and constrain global carbon cycle processes (Francey and Tans, 1987; Ciais et al., 1997; Cuntz et al., 2003a,b). The ^{18}O signal in CO_2 is strongly coupled to the ^{18}O content in soil and leaf liquid water owing to the hydration reaction (Hesterburg and Siegenthaler, 1991). Consequently, the $C^{18}O^{16}O$ signal exhibits dynamic diurnal variations associated with daytime ^{18}O enrichment of leaf water due to transpiration, which leads to a significant departure from the soil water ^{18}O signal (Riley et al., 2003; Bowling et al., 2003a). Given these strong signal differences, $C^{18}O^{16}O$ has been used as a tracer to separate soil respiration from foliar respiration (Mortazavi and Chanton, 2002) and partitioning of F_N into F_P and F_R (Yakir and Wang, 1996). The use of $C^{18}O^{16}O$ for flux partitioning may be particularly advantageous because the $^{13}CO_2$ signatures of F_R, F_P and F_N may be relatively similar or even indistinguishable for many ecosystems (Bowling et al., 2001; Ogée et al., 2003; Lai et al., 2003; Zhang, in press).

The use of $C^{18}O^{16}O$ may also provide an opportunity to quantify the impact of land use change on regional CO_2 exchange. Indeed ^{18}O enrichment of CO_2 in leaves varies among C_3 and C_4 species due to the relative extent of CO_2–H_2O equilibration related to carbonic anhydrase (CA) activity (Gillon and Yakir, 2001). Isotopic equilibration is nearly complete in C_3 species, while lower CA activity in C_4 species can lead to a significant departure from full equilibration. Such differences provide a means to evaluate how land use change is impacting the $C^{18}O^{16}O$ content of the atmosphere. Therefore, quantifying atmospheric variations in the $C^{18}O^{16}O$ signal and estimating the oxygen isotope signature of flux components (F_R, F_N, F_P) can allow for an understanding of changes in regional CO_2 exchange (Farquhar et al., 1993) associated with land management and global biological activity related to climate variations (Ishizawa et al., 2002).

There are two major problems that have limited the use of ^{18}O as a tracer for ecosystem–atmosphere CO_2 exchange. First, estimating end members (isotope signatures of CO_2 flux components) has proven difficult because of the strong spatial heterogeneity at the sub-ecosystem scale and dynamic variation among components at short time scales (i.e. min to hr). Second, the strong influence of water cycle processes on the oxygen isotopic composition of CO_2 demands detailed knowledge of the isotopic composition of soil water, leaf water, and water vapor in canopy air (Amundson et al., 1998; Sternberg et al., 1998; Mortazavi and Chanton, 2002; Bowling et al., 2003b; Ogée et al., 2004).

To date, the majority of CO_2 isotope studies have relied on flask sampling and mass spectrometry methods (Yakir and Wang, 1996; Bowling et al., 1999; Ogée et al., 2004), which have limited the number and frequency of measurements and may be inadequate to fully characterize the variations of atmospheric CO_2 at important timescales. This is especially true for ^{18}O studies because of the strong observed temporal dynamics (Flanagan et al., 1997). From a practical standpoint, flask sampling is expensive, time consuming, and not well-suited to continuous scalar flux estimation. Recently, Bowling et al. (2003c) adapted a tunable diode laser (TDL) system to measure the isotopomers, $^{13}CO_2$ and $C^{16}O_2$. This advance has permitted continuous sampling so that atmospheric fluxes can be better quantified (Griffis et al., 2004). While the new technology still requires refinement of the sampling system, in terms of improved pressure and flow control, the increased temporal resolution should provide better information on the variability and controls on key isotope parameters and discrimination mechanisms. Furthermore, a number of ecosystem–atmosphere models are beginning to include isotope flux process algorithms so that local studies can be extended to regional scales. As a result, there is an increasing need for suitable isotope data for testing and improving these new algorithms (Riley et al., 2003; Ogée et al., 2004). A combination of TDL and micrometeorological measurements should play a key role in addressing these emerging needs.

The objectives of this paper are, therefore, to:

1. Evaluate the performance of the TDL methodology for continuous mixing ratio measurement of the isotopomers $C^{18}O^{16}O$ and $C^{16}O_2$.
2. Demonstrate the feasibility of measuring $C^{18}O^{16}O$ and $C^{16}O_2$ exchange above an agricultural ecosystem using the flux-gradient method.
3. Estimate canopy-scale photosynthetic $C^{18}O^{16}O$ discrimination from direct measurement of net ecosystem CO_2 exchange and its isotopic signature to

evaluate the potential of the TDL technique for ecosystem–atmosphere investigations of discrimination mechanisms and flux partitioning.

2. Material and methods

2.1. Study site

The experiments were conducted at the University of Minnesota, Rosemount Research and Outreach Center (RROC) located 20 km south of the St. Paul Campus. Measurements were performed periodically from March 2004 to April 2005 and included a broad range of environmental conditions. A nearly continuous time series (19 days) was obtained following snowmelt in spring 2004, while flask sample collection and analysis with a mass spectrometer was compared to the TDL at shorter intervals over the period spring 2004 to spring 2005. Field conditions ranged from a bare soil to a full soybean (*Glycine max*) canopy.

2.2. TDL analyzer and calibration

A detailed description of the TDL analyzer (TGA100 Campbell Scientific Inc., Logan, UT, USA) and its configuration for $^{13}CO_2$ stable isotopomer applications is provided by Bowling et al. (2003c). Its modification for water vapor stable isotope measurement can also be found by Lee et al. (2005). The TDL analyzer used in this study has been operational since November 2002 to study diurnal and seasonal dynamics of carbon isotopic CO_2 exchange in a C_3/C_4 managed ecosystem. We have reconfigured the system for a few brief campaigns to measure oxygen isotope ratios of CO_2. Here we provide a short description of this system and detail the modifications for the measurement of $C^{16}O_2$ and $C^{18}O^{16}O$.

In these experiments we selected absorption lines for $C^{16}O_2$ and $C^{18}O^{16}O$ at wavenumbers of 2308.225 and 2308.416 cm^{-1}, respectively. These lines were selected because of their similar effective line strengths (i.e. the line absorption strength is similar with respect to relative natural abundance), close proximity, and because there is also a nearby absorption line for $^{13}CO_2$ measurements (2308.171 cm^{-1}). Ideally, each absorption line should have identical effective strength, thereby reducing errors related to the non-linear response of the sample and reference detectors. In this case, the effective line strengths of $C^{16}O_2$ and $C^{18}O^{16}O$ are better matched than previous TDL measurements of selected $C^{16}O_2$ and $^{13}CO_2$ absorption lines (Bowling et al., 2003c; Griffis et al., 2004). The separation of these absorption lines is, however, greater (0.191 cm^{-1} compared to 0.054 cm^{-1}) than the $C^{16}O_2$ and $^{13}CO_2$ lines. Recently, Bowling et al. (2005) selected a stronger pair of absorption lines for higher precision $C^{16}O_2$ and $^{13}CO_2$ (2293.881 and 2294.481 cm^{-1} with a relatively large separation of 0.600 cm^{-1}) measurements. They demonstrated the accuracy of the TDL for carbon isotope ratios by using four calibration tanks, ranging from 353.3 to 477.4 μmol mol^{-1}, but noted the possibility of non-linearity outside of that range. A co-linearity test is described later to examine these potential effects.

Calibration of the TDL requires standard gases with known mixing ratios of $[C^{16}O_2]$ and $[C^{18}O^{16}O]$. These values were derived from standard gases of known total $[CO_2]$ and oxygen isotope ratio from the following:

$$[CO_2] = [C^{16}O_2] + [C^{18}O^{16}O] + f[CO_2] \quad (1a)$$

$$R_a = [^{18}O]/[^{16}O] = 0.5 \times [C^{18}O^{16}O]/[C^{16}O_2] \quad (1b)$$

$$[CO_2](1-f) = [C^{16}O_2](1 + 2R_a) \quad (1c)$$

$$R_a = R_{VPDB}(1 + \delta_a/1000) \quad (1d)$$

where $[CO_2]$ is the total mixing ratio including all isotopomers, f the fraction (0.01185) of CO_2 containing all isotopomers other than $C^{16}O_2$ and $C^{18}O^{16}O$ and is based on the natural isotopic abundances used for the high-resolution transmission molecular absorption database (HITRAN) (De Bièvre et al., 1984). R_a is the molar ratio of the heavy to light isotope of the sample and the factor, 0.5, accounts for the two atoms of oxygen in CO_2 and ignores the presence of doubly substituted isotopomers such as $^{12}C^{18}O^{18}O$, which are present in very small quantities. R_{VPDB} is the $^{18}O/^{16}O$ standard molar ratio, 0.002088349077 (Vienna Peedee Belemnite or VPDB-CO_2 scale, Allison et al., 1995) defined such that NBS19 (NIST Reference Material 8544 with CO_2 generated from the calcite using 100% phosphoric acid at 25 °C) is exactly −2.2‰ relative to the VPDB-CO_2 scale, δ_a is the oxygen isotope relative abundance and is obtained from, $\delta_a = (R_a/R_{VPDB} - 1) \times 1000$, reported in parts per thousand (per mil, ‰). The mixing ratios, $[C^{16}O_2]$ and $[C^{18}O^{16}O]$ can be obtained from:

$$[C^{16}O_2] = [CO_2](1-f)/(1 + 2R_{VPDB}(1+\delta_a/1000)) \quad (1e)$$

$$[C^{18}O^{16}O] = [CO_2](1-f) - [C^{16}O_2] \quad (1f)$$

Primary standards were obtained from the National Oceanic and Atmospheric Administration–Climate

Monitoring and Diagnostics Laboratory (NOAA–CMDL). Calibration values for Tank A were $\delta^{18}O = -2.90‰$ (VPDB-CO_2 scale) with [CO_2] of 348.61 μmol mol^{-1}. It should be noted that determining the oxygen isotope ratio values of the standard calibration tanks from mass spectrometry requires an ion correction procedure to account for isotopomers ($^{13}C^{17}O^{16}O$ and $C^{17}O_2$) that have the same mass as $C^{18}O^{16}O$. The details of the ion correction procedure can be found in Allison et al. (1995), see Eqs. (12)–(15), and the Appendix of Verkouteren and Lee (2001). In the case of TDL measurements these corrections are not necessary because unique absorption lines can be found for each CO_2 isotopomer. Using Eqs. (1e) and (1f) we calculated [$C^{16}O_2$] and [$C^{18}O^{16}O$] values of 343.05 and 1.43 μmol mol^{-1}, respectively. Tank B values of these quantities were −14.89‰, 568.44, 559.40 and 2.30 μmol mol^{-1}, respectively. Sample mixing ratios of each isotopomer were measured using the TDL and corrected using a two-point gain and offset calibration procedure using the above standards (Bowling et al., 2003c). The oxygen isotope ratio of atmospheric CO_2 in delta-notation is

$$\delta_a = (R_a/R_{VPDB} - 1) \times 1000$$
$$= (0.5 \times [C^{18}O^{16}O]/[C^{16}O_2]/R_{VPDB} - 1) \times 1000 \quad (2)$$

where [$C^{18}O^{16}O$] and [$C^{16}O_2$] are the calibrated mixing ratios of the sample air. Note that some experiments were carried out using secondary standards propagated from the above CMDL standards.

2.3. TDL sampling system

The TDL sampling system used in this study is derived from the one of Griffis et al. (2004). It has been slightly modified from the original configuration to add a sample inlet for ^{18}O measurements and to allow samples to be collected in flasks for mass spectrometry analysis. At the beginning of the experiment a sample inlet was located 0.1 m above a bare soil surface with patchy snow cover. The height of the inlet above the soil surface was varied during the growing season to accommodate changing canopy height. The inlet consisted of a Swagelok stainless steel filter (SS-4F-7, 7 μm sintered element filter, Swagelok, OH, USA) followed by Synflex tubing (Synflex Type 1300, Aurora, OH, USA) connecting the inlet to an eight-valve custom manifold. A critical flow orifice (Model D-7-BR, O'Keefe Controls Co., Monroe, CT, USA) was used at the manifold to set the flow rate to 0.26 l min^{-1}. Normally the orifice would be placed immediately downstream of the filter to reduce the pressure in the inlet tube, thereby avoiding condensation. For this experiment the orifice was placed at the manifold to allow sample flasks to be filled at ambient pressure. A magnesium perchlorate trap at the inlet dried the air sample to prevent condensation and the resultant oxygen isotope exchange between the condensed water and the CO_2 in air sample (Gemery et al., 1996). Flow from the manifold was directed through a Nafion Dryer (PD-200T-24-SS, Perma Pure Inc., NJ, USA) located just before the TDL. The sample lines conducted the air streams back to the TDL instrument trailer located at the edge of the field. When obtaining flask samples we used a single sample line that was approximately 25 m in length. Two sample lines approximately 200 m long were used to measure isotopic fluxes with the flux-gradient method described later. A rotary vane vacuum pump (RB0021, Busch Inc., Virginia Beach, VA, USA) pulled the sample and calibration gases through the sample cell at 2.0 kPa. A reference gas of approximately 10% $C^{16}O_2$ and 0.4% $C^{18}O^{16}O$ balanced in air was used at a flow rate of 10 ml min^{-1} through the reference cell to provide a template of the spectral shape of the absorption lines.

The TDL sampling cycle was as follows: (1) CMDL standard Tank A; (2) CMDL standard Tank B; (3) air sample measurement of [$C^{16}O_2$] and [$C^{18}O^{16}O$] above the soil surface at a height of 0.1 m. Within each 2 min cycle the calibration gases were sampled for 30 s each and the atmospheric inlet was sampled for 60 s. This sequence was later changed by adding a second inlet for measuring the flux gradient. In this second experiment each standard was sampled for 20 s and the two inlets were each sampled for 40 s within a 2 min cycle.

2.4. Flask sampling system and mass spectrometer

A flask sampling system was designed to obtain atmospheric samples over a 2 min interval. The flask system shared the same inlet as the TDL sample system, permitting direct comparison of the same air stream between the mass spectrometer and the TDL. Sixteen two-way solenoid valves (EVN-2M-12V, Clippard Instrument Laboratory, Inc., Cincinnati, OH, USA), mounted on an anodized aluminum manifold (15481-6, Clippard Instrument Laboratory, Inc.), were connected to eight 150 ml Teflon-lined stainless steel sample cylinders (304L-HDF4-150-T, Swagelok) with stainless steel quick connects (SS-QC4-B04PM, Swagelok). A data acquisition system (Daqbook 2000X, IOtech Inc., Cleveland, OH, USA) with relay cards (DBK25, IOtech

Inc.) was controlled using DASYLab software (Version 7.0, IOtech Inc.) to select the appropriate sample flask. A manual flask (170 ml custom glass blown flask with Teflon stopcocks) system was also used for collecting air samples for the TDL-mass spectrometer comparison. We note that both flask sampling systems are susceptible to problems related to leakage, condensation, and fractionation, which have potential to degrade the quality of the TDL-mass spectrometer comparison.

Oxygen isotope ratios of CO_2 flask samples were measured using a TraceGas pre-concentration inlet system interfaced to a continuous-flow isotope ratio mass spectrometer (Isoprime TraceGas and Optima, GV Instruments, Manchester, UK). This system involves on-line pre-concentration of flask samples through a liquid nitrogen cryo-focusing trap. A magnesium perchlorate trap and Nafion membrane removed residual water vapor, and CO_2 and N_2O were separated by gas chromatography. The mass spectrometer precision for δ is approximately 0.3‰. All flasks were analyzed sequentially using an auto-sampler. A set of standard flasks (NOAA-CMDL, $\delta^{18}O = -2.90$‰ VPDB-CO_2 scale) was analyzed with each set of sample flasks. Given the relative precision of the mass spectrometer and the TDL, we did not apply the ion correction to the mass spectrometer flask values as recommended by Allison et al. (1995).

2.5. Eddy covariance flux measurements

Eddy covariance measurements included: friction velocity (u_*), sensible heat flux (H), latent heat flux (λE), and net ecosystem CO_2 exchange (F_N). The eddy covariance system consisted of a sonic anemometer-thermometer (CSAT3, Campbell Scientific, Inc.) and an open-path infrared gas analyzer (LI-COR 7500, LI-COR, NE, USA). A detailed description of the measurement system, flux processing, and quality control procedures can be found in Baker and Griffis (2005).

2.6. Isotopic fluxes and keeling mixing model

The flux-gradient (K-theory) method is based on Monin–Obukhov similarity theory and has been shown to work well above the roughness sublayer where horizontal flow is homogeneous and the dispersion is considered to be far-field or random (Monin and Obukhov, 1954; Simpson et al., 1998; Raupach, 1989). In this particular application of measuring stable isotopic fluxes there are two critical assumptions related to similarity: first, the eddy diffusivities (K) of $C^{18}O^{16}O$ and $C^{16}O_2$ are assumed identical; second, the sink/source distributions for both CO_2 isotopomers are also assumed identical. These assumptions should be reasonable for an agricultural ecosystem where the canopy is horizontally homogeneous and confined vertically within a few meters. Provided that the gradient measurement is made above the roughness sublayer, small differences in sink/source distribution of the two isotopomers (i.e. differences in isotope signature between soil and vegetation fluxes) should have little effect on the flux-gradient measurement due to strong mixing.

Here we measured the ratio of the two isotopomer fluxes (*flux ratio* approach) via K-theory (Griffis et al., 2004)

$$F_N^{18}/F_N^{16} = \frac{-K\bar{\rho}_a/M_a\, \mathrm{d}[\overline{C^{18}O^{16}O}]/\mathrm{d}z}{-K\bar{\rho}_a/M_a\, \mathrm{d}[\overline{C^{16}O_2}]/\mathrm{d}z} \tag{3a}$$

where F_N^{18} and F_N^{16} are the $C^{18}O^{16}O$ and $C^{16}O_2$ fluxes, K the eddy diffusivity of CO_2, $\bar{\rho}_a$ the average density of dry air, M_a the molecular weight of dry air, and $\mathrm{d}[\overline{C^{18}O^{16}O}]/\mathrm{d}z$, $\mathrm{d}[\overline{C^{16}O_2}]/\mathrm{d}z$ are the time-averaged mixing ratio gradients of $C^{18}O^{16}O$ and $C^{16}O_2$ measured simultaneously at the same heights. Sample inlets were positioned at the center of the field with a vertical separation of 0.7 m. Assuming similarity in the eddy diffusivity for $C^{18}O^{16}O$ and $C^{16}O_2$, the flux ratio reduces to

$$F_N^{18}/F_N^{16} = \frac{[\overline{C^{18}O^{16}O}]_{z_2} - [\overline{C^{18}O^{16}O}]_{z_1}}{[\overline{C^{16}O_2}]_{z_2} - [\overline{C^{16}O_2}]_{z_1}} \tag{3b}$$

In this experiment the flux ratio was determined from a geometric linear fit (Model II regression) of the 2 min cycle $[C^{18}O^{16}O]$ gradient (y-axis) versus the $[C^{16}O_2]$ gradient (x-axis) to reduce the influence of potential outliers. The flux ratio was obtained using a 60 min moving window (i.e. thirty 2 min averaged gradient values) with a 15 min time step. The slope of the regression represents the flux isotope ratio, F_N^{18}/F_N^{16} and can be converted to delta notation (δ_N) according to

$$\delta_N = (0.5 \times F_N^{18}/F_N^{16}/R_{VPDB} - 1) \times 1000 \tag{4}$$

we note that in the absence of photosynthetic activity δ_N is equal to the oxygen isotope signature of ecosystem respiration (δ_R) provided that CO_2 storage is negligible. In this initial experiment, the error in δ_N became relatively large (>4‰) as $\mathrm{d}[C^{18}O^{16}O]/\mathrm{d}z$ decreased to less than 0.01 μmol mol^{-1} m^{-1}. All error estimates are shown in Section 3.

The Keeling mixing model parameters were obtained from a geometric mean regression of the oxygen isotope ratio of ambient CO_2 (δ_a) versus the reciprocal of the total [CO_2]. When this model is applied to nighttime or non-growing season conditions, the intercept of the linear fit is assumed to represent the flux isotope signature of the source (ecosystem respiration) end member. The relationship will be linear only if the respired CO_2 that is mixed into the atmosphere has a constant oxygen isotope ratio. This technique has proven to be very robust for $^{13}CO_2$ applications (Pataki et al., 2003a), but is noted to be less reliable when applied to ^{18}O measurements. In ecosystems with significant $^{13}CO_2/C^{16}O_2$ variations in the sources at the sub-ecosystem scale, the two end-member Keeling mixing model (Keeling, 1958) has proven robust when applied to nighttime data, because the contribution of each ecosystem component is relatively conservative over time (Yakir and Sternberg, 2000). It is well established, however, that the Keeling mixing model is less reliable at the ecosystem scale when applied to ^{18}O in water vapor or CO_2 because of the greater spatial heterogeneity in the oxygen isotope ratio of the source water in leaves and soil at relatively small spatial scales (i.e. less than the field scale) and dynamic variation among these components at short time scales (i.e. min to hr) (Amundson et al., 1998; Sternberg et al., 1998; Mortazavi and Chanton, 2002; Bowling et al., 2003b; Ogée et al., 2004). As a result, the Keeling approach cannot be used to reliably determine the $C^{18}O^{16}O$ mass balance (Ogée et al., 2004). The ability to measure the mixing ratio and fluxes of $C^{18}O^{16}O$ and $C^{16}O_2$ directly should yield a more robust approach because: (1) flux measurements are less sensitive to changes in the so-called background concentration and isotope composition, which are needed for mixing model analyses; (2) fluxes can be obtained at relatively short time intervals whereas mixing model analyses require significant buildup of the scalar over relatively long time periods, making them susceptible to advective influences; (3) concentration footprints are much greater than flux-gradient or eddy-covariance footprints and may, therefore, be mismatched with the ecosystem flux measurement.

3. Results and discussion

3.1. Concentration and pressure sensitivity

Non-linear errors in the measurement of [$C^{16}O_2$] and [$C^{18}O^{16}O$] can arise from non-linear response in the reference and sample detectors or from the multi-mode output (i.e. emission at undesired frequencies) from the laser. The TGA100 software includes corrections for detector non-linearity and laser multi-moding, however, relatively small residual errors could bias the observed oxygen isotope ratio. Both of these potential sources of error are affected by the choice of absorption lines because of non-ideal laser characteristics. Widely spaced absorption lines require a large change in laser current to step between them. This larger current step is more likely to produce a significant change in the laser's power output or multi-moding. Bowling et al. (2005) used a set of four calibration tanks with well-known [CO_2] and carbon isotope ratio to demonstrate the TDL's linearity over the range of 353.3–477.4 μmol mol^{-1}. We measured an air stream with variable mixing ratio and constant oxygen isotope ratio produced by mixing air from two tanks: one containing 10% CO_2 and the other containing CO_2-free air. This test does not verify the absolute linearity of the TDL, which would require precise calibrated measurement of the mixing ratio of each isotopomer. However, it does verify the co-linearity of the two isotopomers, which is required for their ratio to remain constant. Fig. 1 demonstrates that

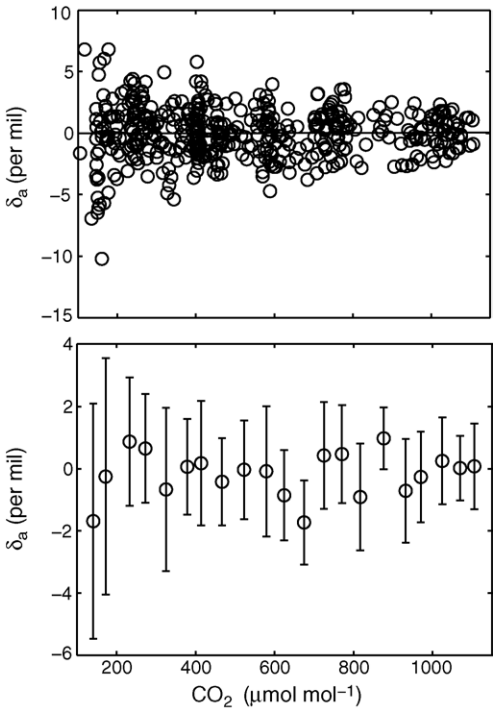

Fig. 1. Co-linearity test illustrating the sensitivity of the oxygen isotope ratio (δ_a) to varying CO_2 mixing ratio. The isotope data are not calibrated and were plotted after removing a constant offset factor. The solid line represents the linear regression and sensitivity (upper panel). The binned data (50 μmol mol^{-1} bin widths) illustrate that the TDL noise tends to increase when CO_2 mixing ratio is less than 200 μmol mol^{-1} (lower panel).

the oxygen isotope ratio was relatively stable over a range of $[CO_2]$ from 100 to 1200 μmol mol^{-1}. The derivative of the linear function shown in Fig. 1 (upper panel) provides an estimate of the non-linearity error of 7.1×10^{-5}‰ for a 1 μmol mol^{-1} change in $[CO_2]$. We expect, therefore, that under most atmospheric conditions the non-linearity error would be insignificant. Further, Fig. 1 (lower panel) also illustrates that at low $[CO_2]$ the noise (standard deviation) in the oxygen isotope ratio tends to increase.

The observed oxygen isotope ratio can also be affected by sample cell pressure. We examined the pressure effect using another TGA100 with similar laser, using the same absorption lines. Sample cell pressure was varied over a broad range (1.5–2.5 kPa) while measuring a tank of compressed air. This experiment was repeated several times over a 3-day period and produced variable results. The oxygen isotope ratio increased, decreased, or varied sinusoidally with a period of approximately 0.5 kPa. The isotope ratio changed by as much as ±0.5‰ for a 0.1 kPa change in pressure. This behavior is likely the result of optical interference caused by multiple reflections within the sample cell. Optical interference produces an offset error that can change over time. For instance, if the length of the sample cell changes (i.e. due to thermal expansion) by one half the laser wavelength, the reflected beam will go through a complete cycle of constructive/destructive interference. The effective path length in the sample cell also depends on the pressure, which influences the index of refraction. A pressure change of approximately 0.5 kPa would change the effective path length for the reflected beam by one wavelength. The offset error resulting from this optical interference is removed by comparing the air sample to calibration tanks. However, if the air sample and calibration tanks are measured at different pressures, the offset error will not be removed properly. For this reason the TDL sampling system is designed to minimize pressure differences. During our field experiments the pressures were typically matched to within 0.01 kPa. Therefore, an uncertainty of 0.05‰ is assigned to the oxygen isotope ratio measurements to account for this pressure effect. We note, however, that the pressure bias nearly vanishes when measuring in a gradient mode, provided the pressure matching is 0.01 kPa or better.

3.2. Measurement precision

We measured a non-calibrated cylinder of compressed air over a period of 11 h using the TDL calibrated against two CMDL standards. This experiment was conducted with the TDL and air cylinders located inside the RROC temperature-controlled research trailer. The measurement precision observed here may not apply to situations where the TDL and air cylinders are maintained in ambient conditions. Fig. 2 shows the calibrated data for each 2 min measurement cycle. After applying a two-point gain and offset correction, we obtained a 2 min measurement precision (1 standard deviation) of 0.09, 0.0004 μmol mol^{-1} and 0.26‰, for $^{12}CO_2$, $C^{18}O^{16}O$, and δ, respectively. The 30 min (i.e. average of fifteen 2 min cycles) measurement precision improved to 0.02, 0.0001 μmol mol^{-1}, and 0.07‰, respectively. These values are comparable to other published results for the TGA100 using absorption lines of similar strength. Precision of the TDL for $^{13}CO_2$ has been reported as 0.24 and 0.06‰ for a 2 and 30 min averaging period, respectively (Bowling et al., 2003c; Griffis et al., 2004). We note that in a recent TGA100 experiment, Bowling et al. (2005) used stronger $C^{16}O_2$ and $^{13}CO_2$ absorption lines and achieved an average 6 min measurement precision for the carbon isotope ratio of 0.06‰. Based on summertime flux-gradient measurements (described later) the

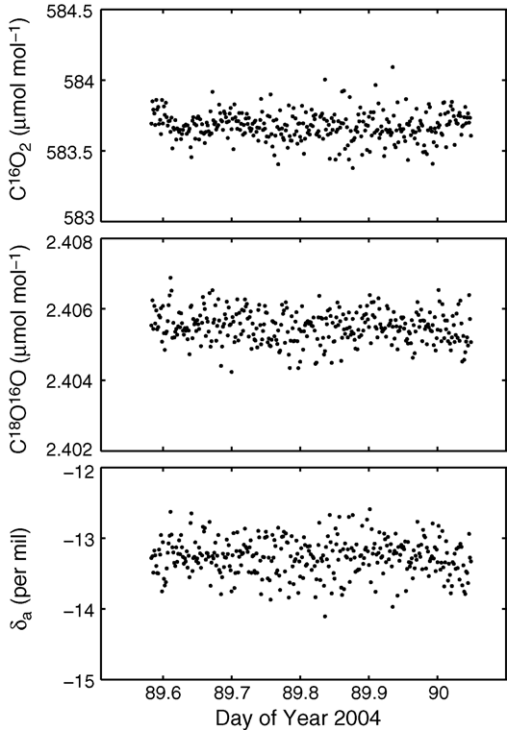

Fig. 2. TDL precision for $C^{16}O_2$ (upper panel), $C^{18}O^{16}O$ (middle panel) and δ_a (lower panel). The data represent 2 min measurement cycles (30 s averages for each sample) of an unknown air cylinder with the TDL calibrated against NOAA-CMDL standards over an 11 h period.

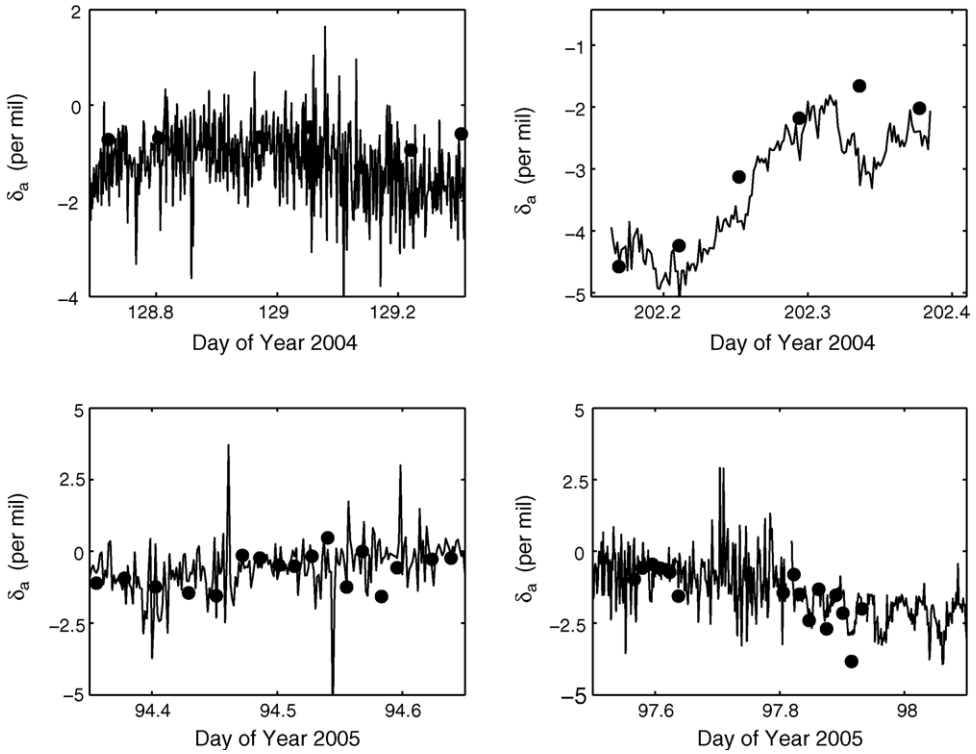

Fig. 3. Temporal variations of δ_a in CO_2 flask samples based on TDL spectroscopy and mass spectrometry. Data were collected on DOY 128–129, 2004 (upper left panel); DOY 202, 2004 (upper right panel); DOY 94, 2005 (lower left panel); DOY 97–98, 2005 (lower right panel). Note that in the upper right panel a 5 L buffer volume was used upstream of the automated flask sampling system.

TDL precision should be adequate for resolving oxygen isotope fluxes at relatively short timescales (i.e. 30 min).

3.3. Mass spectrometer and TDL comparison

Fig. 3 (upper left panel) shows a comparison between TDL and mass spectrometer 2 min averaged values taken over a period of 16 h on DOY 128–129 (May 7–8, 2004) at the RROC field site. Flask samples, with a 2 min residence time, were obtained every 2 h during this period. There was relatively little diel variation as shown in both datasets. The comparison illustrates relatively good agreement: mass spectrometer flask samples averaged −0.77‰ (±0.25), and TDL 2 min samples averaged −0.89‰ (±0.11). Bracketed terms indicate the standard deviation of the sample values. Fig. 3 (upper right panel) illustrates a comparison for DOY 202 (July 20, 2004), also showing relatively good agreement with strong enrichment occurring during the day. The diurnal variation ranged from −5 to −2‰. Note that in this case a 5 L buffer volume was positioned up stream of the flask system, which caused a significant reduction in the TDL noise.

During spring 2005 the manual flask system was used in order to limit the problem related to TDL sample cell pressure transients when using multiple flask switching. In general, better agreement was observed between the TDL and mass spectrometer measurements when using this simplified approach. Fig. 3 (lower left panel) illustrates a comparison for DOY 94 (April 4). The flask sample values were well within the range of the TDL measurements and tracked the observed daytime enrichment, with δ_a exceeding 0‰ by late afternoon. Flask samples were collected during the early afternoon and late evening on DOY 97 (April 7) (Fig. 3, lower right panel). Both the TDL and flask samples reveal the expected pattern of daytime enrichment and nighttime depletion. The nighttime data on DOY 97–98 illustrate a series of oscillations in δ_a related to variability in turbulent mixing.

A 1:1 plot of the data from all valid flask experiments is shown in Fig. 4. The geometric regression indicates relatively good agreement ($y = 1.01x - 0.008$, $r^2 = 0.94$, $n = 88$) between the TDL and mass spectrometer. On average the TDL technique measured δ values that were slightly more negative (0.006‰) than the mass spectrometer values. The mean and standard

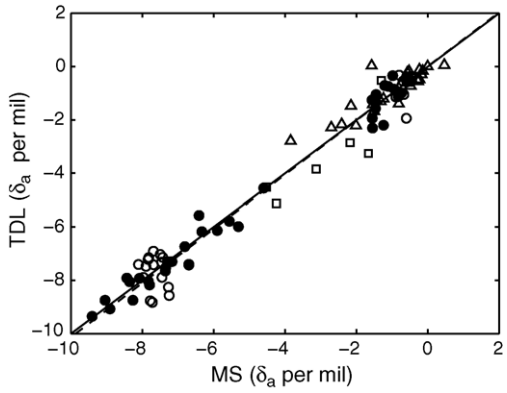

Fig. 4. Geometric regression comparison of δ_a flask samples measured with TDL spectroscopy and mass spectrometry. Closed circles indicate manual glass flask measurements; open circles indicate automated stainless steel flask samples; open triangles indicate manual stainless steel flask samples; open squares represent stainless steel flask samples with a 5 L buffer volume upstream of the automated flask sampling system. The data points represent all valid flask samples collected over the experimental period, March 2004–April 2005.

error for the TDL and mass spectrometer values (rounded to 3 significant digits) were −3.90‰ (±0.35) and −3.90‰ (±0.34), respectively. The mean of the differences (TDL-MS values) and the standard deviation were −0.05 and 0.55‰, respectively. The Kruskal–Wallis test (Matlab, The Mathworks Inc., Massachusetts, USA) indicated no statistically significant difference between the two sample populations (null hypothesis rejected, $p = 0.88$). Further, the mean difference was within the measurement precision (0.3‰) of each technique. Some of the larger differences (>1‰) observed between pairs of samples can be attributed to error associated with TDL sample cell pressure differentials that resulted from having the flask sampling system inline with the TDL system. Sample cell pressure matching for each sample flask (automated system) was extremely difficult to achieve. The manual single flask system provided better results because of the improved sample cell pressure stability.

The standard deviation of the mass spectrometer-TDL differences was 0.10‰ larger than that reported for a $^{13}CO_2$ comparison using similar methodology by Bowling et al. (2003c).They also observed a systematic offset of 1.77‰ in their comparison of TDL and mass spectrometer measurements of $\delta^{13}CO_2$. However, their relatively large difference was attributed to pressure broadening caused by working standards that were balanced in nitrogen and not air. The comparison provided here, and subsequent experiments by Bowling et al. (2005) with calibration standards balanced in air, further supports that conclusion. Lee et al. (2005) also found good agreement between TDL and mass spectrometer measurements of ^{18}O in water vapor. Their TDL measurements differed from the cold-trap – mass spectrometer technique by −0.36‰ with a standard deviation of 1.43‰. The larger standard deviation was attributed to the difficulties of condensing-out all of the flask sample water vapor using the cold-trap technique.

3.4. Mechanisms influencing the temporal variations of δ_a

Nearly-continuous TDL measurements were obtained from DOY 82 (March 22, 2004) to DOY 100 (April 9, 2004) following spring snowmelt (Fig. 5). The averaged air temperature and ecosystem respiration rate were 6.8 °C and 1.1 μmol m^{-2} s^{-1}. In general, δ_a ranged from about −4 to +1‰ and was within the observed atmospheric values reported for ecosystem and regional studies (Flanagan et al., 1997; Lloyd et al., 2002; Styles et al., 2002; Ogée et al., 2004) and within the range of observed global values (Trolier et al., 1996). Over the course of the 19-day measurement period there was no statistically significant trend in δ_a.

The time series plot (Fig. 5) and the 24 h ensemble averages (Fig. 6) suggest a number of mechanisms that can influence the temporal variation of δ_a in surface air. The research site is at the urban-rural interface and is at times subject to the influence of urban pollution. The large spikes in $[CO_2]$ (>400 μmol mol^{-1}) during this time of the year are indicative of combustion plumes (Lee et al., 1991), causing relatively low δ_a values. For example, on DOY 85, 86, 95, and 96 we observed Keeling plot intercepts with values ranging between −15 and −18‰, which is characteristic of the theoretical combustion derived signal (i.e. −17‰) (Kroopnick and Craig, 1972). We note, however, that these Keeling plots showed considerable scatter resulting in weak r^2 values. Pataki et al. (2003b) used an isotopic mass balance approach to partition the production of urban CO_2 in Salt Lake City, UT, USA. Their results indicated that the combustion signal differed from the theoretical value of −17‰ and that variation in wintertime $[CO_2]$ was dominated by natural gas and gasoline burning. In environments located at the urban/rural interface the combustion signal has great potential to contaminate mixing line analyses of ecosystem exchanges at any time of year.

Fig. 6 illustrates the diurnal ensemble average of friction velocity (u_*), latent heat flux (λE) and δ_a over

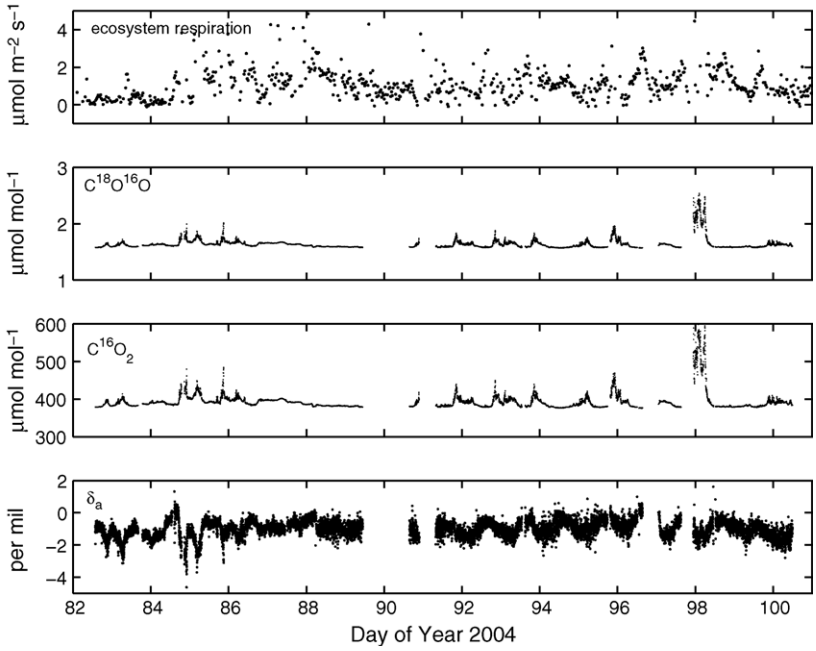

Fig. 5. Time series of ecosystem respiration, the isotopomer mixing ratios of $C^{16}O_2$ and $C^{18}O^{16}O$, and the oxygen isotope ratio (δ_a) measured over a 19-day period (DOY 82–100) in 2004.

the 19-day period. Strong daytime turbulence and increased λE flux were generally associated with ^{18}O enrichment of atmospheric CO_2 near the surface. However, δ_a was only weakly correlated ($r^2 = 0.29$) with F_N (i.e. biological activity). The main cause of the δ_a diurnal pattern was the expansion of the daytime boundary layer and entrainment of relatively unpolluted and hence more ^{18}O enriched air from above the morning surface inversion. Theoretically, the daytime ^{18}O enrichment can result from soil CO_2 equilibration with near surface soil water enrichment caused by soil evaporation (Amundson et al., 1998; Riley et al., 2002), although the magnitude of this effect is not known at this time because of lack of information on the soil water ^{18}O content.

Fig. 7 shows a magnified view of a portion of the time series presented above. It reveals an upward ramp in the oxygen isotope ratio beginning midday on DOY 87, followed by a sudden step change early on DOY 88. There are at least two potential factors that may be involved. It rained on both days (11.3 mm on DOY 87/March 27, 2004 and 0.5 mm on DOY 88/March 28, 2004) and there was also a change in air mass source. Back trajectory analysis, using the NOAA HYSPLIT model (Draxler and Rolph, 2003) revealed that prior to March 28 the source air originated from the Gulf of Mexico. By midday on March 28 the source air could be tracked back to southern Manitoba and North Dakota. This cold frontal system resulted in a change of wind direction from ESE to WNW and was accompanied with strong decreasing air temperature. Such dramatic changes in air mass source could be responsible for the rapid change in the oxygen isotope ratio of CO_2 early on DOY 88. Helliker et al. (2002) also observed similar changes in the oxygen isotopic signature of water vapor associated with changes in wind direction and air mass. The more gradual change beginning on DOY 87 may reflect a change in soil respiration in response to the initial wetting caused by the first rain event, which was relatively large, and increasing air temperature. Unfortunately, no precipitation water was archived to confirm the isotope ratio of the precipitation related to this event. Based on historical datasets (1989–1993) the precipitation $^{18}O/^{16}O$ isotope ratio has shown considerable variation, ranging from −17 to −0.2‰ and averaging −8.4‰ (VSMOW scale) (United States Network for Isotopes in Precipitation, USNIP, www.nrel.colostate.edu/projects/usnip/). The strong variation observed is dependent on the precipitation type and back trajectory of the air mass (source water). In general, a precipitation event is more likely to produce a short-term decrease (relative depletion) in the oxygen isotope ratio of soil respiration – providing further support that the observed step change in δ_a was related to the air mass source.

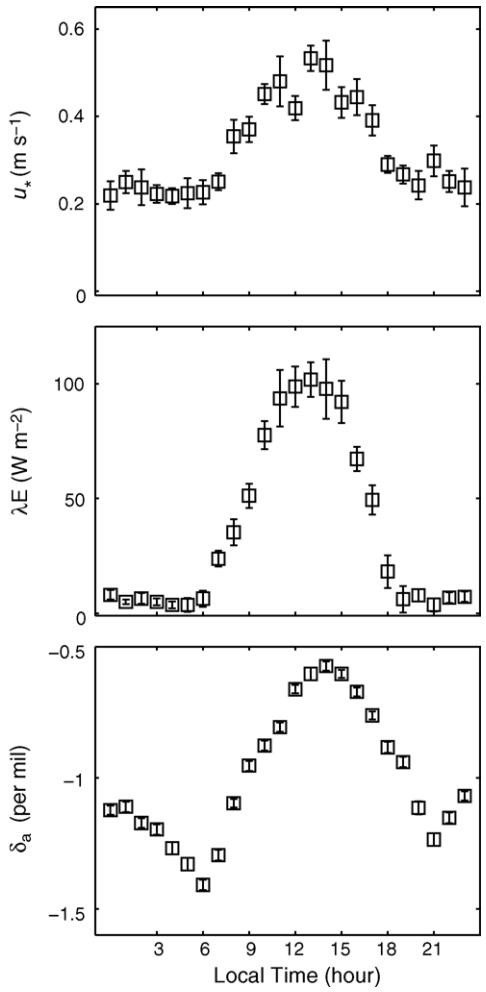

Fig. 6. Diurnal values of friction velocity (u_*, upper panel), latent heat flux (λE, middle panel) and the oxygen isotope ratio of CO_2 (δ_a, lower panel) for the 19-day period (DOY 82–100) in 2004.

3.5. Temporal variations in the isotopic signature of ecosystem respiration

The Keeling mixing model was used to estimate the isotopic signature of soil respired CO_2 (δ_R) for the period DOY 82–100. The experiment represents a relatively simple test case with homogeneous bare soil conditions at RROC. The air intake level was positioned very close to the ground (at 0.1 m above the surface) to limit the concentration source footprint. However, we recognize that even at this height the ^{18}O signal is subject to the influences of advection and combustion plumes. Keeling parameters were computed at time intervals ranging from 2 to 48 h in order to examine temporal scale variations and the influence of environmental conditions on the parameters. Realistic parameter values (statistically significant results) were

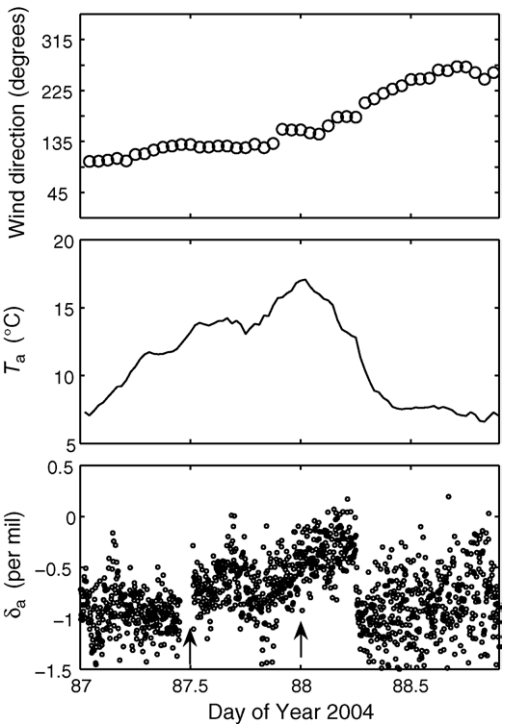

Fig. 7. Influence of air mass source and precipitation on the oxygen isotope ratio (δ_a) of ambient air. δ_a was measured approximately 10 cm above a bare soil surface (lower panel). Arrows indicate precipitation events. Air temperature (middle panel) was measured at 3 m above the surface. Wind direction (upper panel) was measured at a height of 10 m above the soil surface.

obtained for only 32% of the 24 h cases and 30% of the 48 h cases. As the temporal scale was refined toward 2 h intervals, the mixing model failure rate increased. Only 7% of the 2 h cases produced realistic parameter estimates. These observations reinforce that the Keeling function cannot be used reliably to obtain the eddy $C^{18}O^{16}O$ isoflux (mass balance), which is typically derived from half-hourly time intervals.

The coefficient of determination for each model fit was used as a diagnostic parameter to better understand the conditions for which the data conformed to the linear mixing model assumptions applied at each temporal scale. We considered the following factors: concentration range, atmospheric stability, flux footprint, friction velocity, and latent heat flux. Flux footprint was estimated using the Schuepp et al. (1990) model – modified to account for stability corrections (Blanken et al., 2001). None of the above factors could be directly linked to the quality of the Keeling plot analyses. For instance, at the 12 h temporal scale we observed six periods with δ_R values characteristic of a combustion signal (parameter values

not statistically significant). Range of $[CO_2]$, which has been shown to have an important influence on estimating the carbon isotope signature of respiration (Pataki et al., 2003a), did not have a significant influence on the ^{18}O application of the mixing model. For example, there were periods when the temporal range of $[CO_2]$ was large (>80 μmol mol^{-1}), but the Keeling parameters were poorly constrained. At the 24 and 48 h temporal resolution the most important factor influencing the quality of the Keeling plots was u_* – with lower u_* producing slightly better results. Lower friction velocity is typically associated with poor mixing and larger range of ambient $[CO_2]$, but extended concentration footprints. These results indicate that the ecosystem–atmosphere $C^{18}O^{16}O$ exchange is complex and even in this ''simple'' case, influenced by more than two pools (i.e. soil, combustion, and background air) over a variety of time scales.

The isotope signatures of respiration, computed from the ''best fit'' cases, had values ranging between −35 and −33‰, which is consistent with cold season (October) observations made by Flanagan et al. (1999) in a boreal forest. Their ecosystem-scale respiration observations ranged from −16.2‰ during summer to −31.3‰ during October when temperatures were near freezing. The greater depletion in October was directly attributed to decreased leaf respiration and precipitation events that were depleted in ^{18}O. Furthermore, data from USNIP illustrate that precipitation events in Minnesota are considerably more depleted (negative) in ^{18}O during the winter compared to summer.

3.6. Temporal variations in the isotopic signature of net ecosystem CO_2 exchange

Growing season gradient measurements of $[C^{18}O^{16}O]$ and $[C^{16}O_2]$ were made for a 24 h period from midday DOY 251 to midday DOY 252 (September 7 to September 8, 2004) above a fully developed soybean canopy. Midday $[C^{16}O_2]$ and $[C^{18}O^{16}O]$ gradients, for $u_* > 0.1$ m s^{-1}, were 0.98 and 0.004 μmol mol^{-1} m^{-1}, respectively and were significantly greater than the 2 min measurement precision (i.e. 0.09 and 0.0004 μmol mol^{-1}) of the TDL analyzer. The δ_a signal measured at the lowest inlet is shown in Fig. 8 along with λE and F_N. Nighttime δ_a values were relatively depleted in $C^{18}O^{16}O$ (−5‰) while midday values were relatively enriched by approximately 2‰. This diurnal variation compares well with growing season measurements made over a pine stand (*Pinus pinaster*) in Bordeaux, France by Ogée et al. (2004) and during the non-growing season

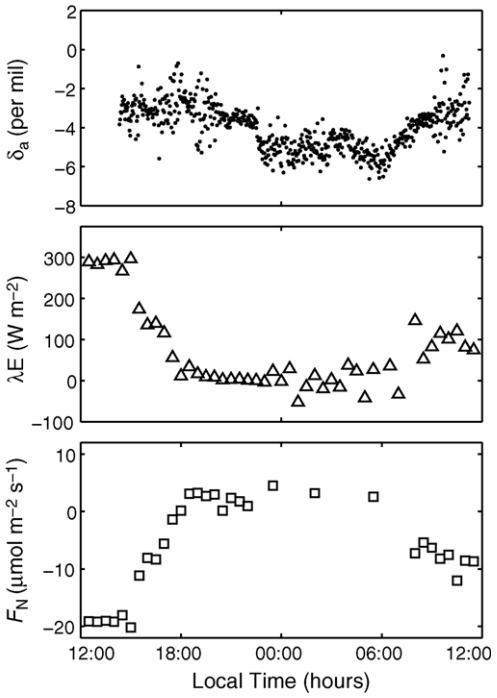

Fig. 8. Time series of the oxygen isotope ratio of CO_2 (δ_a), latent heat flux (λE), and net ecosystem CO_2 exchange (F_N) measured above a soybean canopy for a 24 h period from DOY 251 (September 7) to DOY 252 (September 8), 2004. δ_a values represent TDL 2 min cycle data. λE and F_N represent half-hourly values measured using the eddy covariance approach.

(Fig. 5). Based on these data and the 19 day time series in 2004 the diurnal amplitude of δ_a appears to be less pronounced than for $^{13}CO_2$. Daytime growing season enrichment is expected due to erosion of the nocturnal boundary layer and also from the retro-diffusion of CO_2 via photosynthesis (Yakir and Sternberg, 2000).

The nighttime Keeling plot for this time series showed a relatively good fit to the data ($r^2 = 0.59$) compared to many other nighttime periods that we examined. The nighttime estimate of δ_R was −10.3‰ with a standard error of ±0.32‰. The isotope flux ratio for the same time period resulted in a δ_R value of −12.1‰ with a standard error of ±1.6‰ ($r^2 = 0.99$). Fig. 9 (top panel) illustrates that nighttime F_R was relatively depleted in $C^{18}O^{16}O$, with δ_R varying by about 8‰ over the nighttime period (mean −9‰, S.E. ± 1.4‰). Near midday the flux isotope ratio varied from −40 to −20‰ as a result of photosynthesis and the retro-flux of CO_2. Based on sign convention a negative δ_N value for daytime F_N denotes enrichment of the surface layer in $C^{18}O^{16}O$. There is a very interesting transition to positive δ_N near sunset and following sunrise when λE and F_N were small. Positive δ_N values

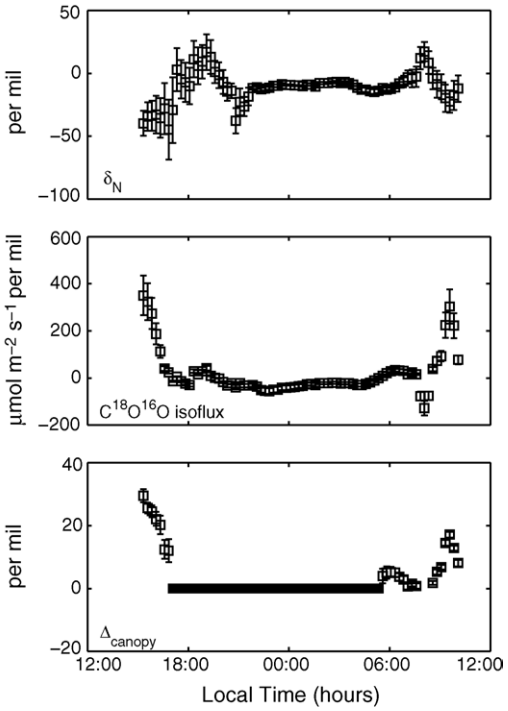

Fig. 9. Oxygen isotope ratio of net ecosystem CO_2 exchange (δ_N, top panel) and the $C^{18}O^{16}O$ isoflux (middle panel) measured above a soybean canopy for a 24 h period from DOY 251 (September 7) to DOY 252 (September 8), 2004. The flux ratio of F_N was obtained using a 60 min moving window with a 15 min time step. The error bars represent the standard error of the δ_N estimate. The isoflux values (middle panel) were obtained by multiplying F_N and δ_N. F_N values were interpolated between half-hourly periods using a cubic spline method. The error bars represent the maximum probable error obtained via error propagation for isotopic flux measurements (Griffis et al., 2004). Canopy-scale ^{18}O photosynthetic discrimination (bottom panel) was estimated using an inversion method. The error bars represent the maximum probable error obtained by examining the partial derivatives of Eq. (5) with respect to each variable evaluated at its mean value. We assumed relative errors of 25% for the isoflux terms and the estimate of gross ecosystem photosynthesis. Canopy-scale photosynthetic discrimination was set to zero (black solid line) for periods when F_N was positive and when photosynthesis approached zero.

can only be explained by a change in the sign of the isotope signature of ecosystem respiration (i.e. soil or leaf respiration). Model results from Riley et al. (2002) indicate that the isotope signature of soil and leaf respiration can change sign at short time-scales (min to hr). Recently, Cernusak et al. (2004) observed dramatic enrichment (+284‰, VPDB-CO_2 scale) in the isotopic signature of dark leaf respiration caused by the diffusion of CO_2 into leaves and its subsequent equilibration with ^{18}O in leaf water and diffusion back to the atmosphere. In this process, the CO_2 is exchanged without impacting the net flux. We hypothesize that the daytime positive values of δ_N occurred when daytime leaf respiration had an isotope signature that was positive in sign because of highly ^{18}O enriched leaf water. These observations further highlight the need for simultaneous and frequent observation of the isotope signature of leaf water and water vapor.

As expected, the 15 min flux ratio estimates illustrate that the diurnal variation is very dynamic as a result of strong changes in transpiration and photosynthesis. The $C^{18}O^{16}O$ isoflux (i.e. the product of δ_N and F_N) is shown in Fig. 9 (middle panel). During daytime conditions the isoflux was generally positive (i.e. atmospheric ^{18}O enrichment) and ranged up to 400 μmol m^{-2} s^{-1} ‰. To date, few observations of the $C^{18}O^{16}O$ isoflux exist (Bowling et al., 1999; Riley et al., 2003; Ogée et al., 2004; Kato et al., 2004) and all of these experiments have been of limited duration (a few days or less) or have depended heavily on modeled discrimination assumptions. Results reported by Bowling et al. (1999) for a Tennessee deciduous forest ranged up to 250 μmol m^{-2} s^{-1} ‰ during daytime conditions when using the so-called EC/flask method, but often exceeded 400 μmol m^{-2} s^{-1} ‰ when using the relaxed eddy accumulation technique. Ogée et al. (2004) found that the EC/flask and Keeling transfer approach was unreliable for estimating the isoflux of $C^{18}O^{16}O$ at the Bordeaux forest site. Values from their flux-gradient method showed considerable diurnal scatter with maximum values of about 400 μmol m^{-2} s^{-1} ‰. Modeled midday isoflux values by Riley et al. (2003) reached 300 μmol m^{-2} s^{-1} ‰ over the tallgrass prairie site. While there remains scant $C^{18}O^{16}O$ isoflux data available for comparison, the results reviewed here show similar magnitude and sign over the diurnal period.

For comparison with field-scale and leaf-level photosynthetic ^{18}O discrimination (Δ) studies, and to provide a diagnostic check on our flux ratio measurements, we inverted and calculated Δ_{canopy} from the conservation equation for $C^{18}O^{16}O$ exchange (Ogée et al., 2004)

$$\delta_N F_N = (\delta_a - \Delta_{canopy})F_P + \delta_R F_R \quad (5)$$

where the left-hand-side of Eq. (5) represents the isoflux. To a very close approximation, $\Delta_{canopy} = \delta_a - \delta_p$, the difference between the isotope ratio of the ambient air (δ_a) and the isotopic signature of the photosynthetic flux (δ_p). Δ_{canopy} is the canopy-scale photosynthetic discrimination against $C^{18}O^{16}O$ resulting from CO_2 diffusion into the leaves and isotopic equilibration of ^{18}O in CO_2 with leaf water via CA activity. The retro-

diffusion (retroflux) of unfixed CO_2 out of the leaf causes $C^{18}O^{16}O$ enrichment of the atmosphere (Yakir and Sternberg, 2000). The fluxes F_R and F_P were estimated by assuming that the nighttime F_N is equal to F_R and then subtracting F_R directly from daytime F_N to obtain F_P. An important limitation of the above approach is that we assume δ_R to be constant. In reality, it is likely to vary substantially during the daytime due to a number of complex factors (Ogée et al., 2004). Two key factors include leaf water evaporative enrichment (Bowling et al., 2003a; Cernusak et al., 2004, 2005) and soil CO_2 effluxes that are only partially equilibrated with soil water following the invasion and retrodiffusion process (Miller et al., 1999; Tans, 1998). Consequently, these preliminary estimates of Δ_{canopy} may be somewhat crude, yet in this particular case they illustrate that the measurements follow mass balance. The daytime discrimination values are shown in Fig. 9 (lower panel) and ranged from 0.6‰ during early morning to 29.5‰ near mid-afternoon (full sun) with a mean and standard deviation of 10.5 and 8.8‰, respectively. Our observations for this short time period suggest that midday isotopic disequilibrium (the difference between δ_P and δ_R ~20‰), is large, which has been observed in other ecosystems (Ogée et al., 2004) and was significantly greater than the $^{13}CO_2$ isotopic disequilibrium (3‰) observed during midsummer for our corn–soybean rotation ecosystem (Griffis et al., 2005). Because the mass balances of $C^{18}O^{16}O$ and $C^{16}O_2$ are effectively decoupled as a result of differences in the isotope signature of soil and leaf water, continuous flux ratio measurements should provide a powerful constraint on F_N partitioning (Ogée et al., 2004).

Canopy-scale Δ_{canopy} values obtained by Riley et al. (2003) for the tallgrass prairie site ranged from 9 to 24‰ for seven midday measurements (DOY 127–203) during 2000. Their 2 days of intense diurnal measurements (DOY 191–192) showed Δ_{canopy} values ranging from about 6 to 40‰. Wang et al. (1998) made detailed leaf-level measurements in the field and laboratory for an arbitrary range of plant species and showed that Δ_{leaf} values ranged from 13 to 60‰ for light-levels greater than 500 μmol photons m^{-2} s^{-1} and vapor pressure deficits less than 3 kPa. The differences were related to the oxygen isotope ratio of leaf water, which varied according to specific species characteristics. Global estimates of Δ_{canopy} for C_3 and C_4 species, used in large scale simulation models, have been approximated at 15 and 7‰, respectively. Such estimates are highly sensitive to the extent of CO_2–leaf–water equilibration via CA activity (Gillon and Yakir, 2001), which varies significantly among species. Unfortunately, few studies have directly quantified canopy-scale $C^{18}O^{16}O$ photosynthetic discrimination under field conditions, which is needed for improving these large scale simulation models.

4. Conclusions

At the present time quantifying the diurnal and seasonal dynamics of these key isotope parameters and discrimination processes at the ecosystem scale is required to advance our understanding of land-atmosphere CO_2 exchange processes so that we may distinguish changes in atmospheric CO_2 driven by climate variation, land use change, and anthropogenic emissions. We recognize that the Keeling method is not ideal for estimating the oxygen isotope signature of respiration or determining the isoflux of the net ecosystem CO_2 exchange because of its sensitivity to sub-field-scale heterogeneity, advection, and contamination from combustion plumes. The experimental approach and data presented in this paper represents a first attempt to obtain continuous flux-gradient measurements of $C^{18}O^{16}O$ exchange at the field-scale using a TDL technique. The methodology can be used to obtain the isotope signatures of flux components (end members) at relatively high temporal resolution to better investigate discrimination mechanisms and flux partitioning. The results confirm the capability of the system to make continuous mixing ratio and flux measurements of the $C^{16}O_2$ and $C^{18}O^{16}O$ isotopomers. Combined with TDL isotopomer water vapor measurements (Lee et al., 2005), there will exist a new opportunity to resolve a number of key issues related to the extent of equilibration between leaf water and CO_2 and other discrimination processes.

Our analysis highlights that the interpretation of the ^{18}O signal at this high temporal resolution will require a number of supporting measurements. Routine sampling of the isotope ratio of precipitation and soil water is required to better understand the dynamics of the respiration flux isotope signature and to determine the extent of isotopic equilibrium with near-surface soil water. The isotope ratio of leaf and stem water can be used to help determine ^{18}O photosynthetic discrimination. Further, the in situ measurement of canopy water vapor isotopomers using the TDL technique offers a potentially powerful method to observe and keep track of changes in the oxygen isotope ratio of these key components. Future research involving simultaneous measurement of ^{18}O flux ratios in CO_2 and water vapor is needed to evaluate the potential of using this type of methodology to isotopically partition net ecosystem

CO_2 exchange and to resolve differences in canopy-scale photosynthetic discrimination between C_3 and C_4 canopies.

In conclusion, we have demonstrated that:

1. Two-minute precision (1 standard deviation) for [$C^{18}O^{16}O$], [$C^{16}O_2$] and δ was 0.0004, 0.09 μmol mol^{-1}, and 0.26‰, respectively. Such precision is adequate for resolving vertical gradients and determining the flux isotope ratio of ecosystem exchange above agricultural ecosystems.
2. TDL measurement of the air CO_2 isotope ratio and mass spectrometer analysis of flask samples showed relatively good agreement ($r^2 = 0.94$) with a standard deviation of 0.55‰ for the residual values.
3. Diurnal amplitude in atmospheric CO_2 oxygen isotope ratio was typically 2–3‰ related to boundary layer dynamics and net ecosystem CO_2 exchange. The TDL system was capable of detecting the influence of combustion plumes and retroflux of CO_2 via photosynthesis on short-term variations in the oxygen isotope ratio.
4. Hourly isotope flux ratio measurements of nighttime ecosystem respiration ranged from −15 to −7‰ and daytime net ecosystem CO_2 exchange ranged from −40 to −20‰.
5. Canopy-scale photosynthetic $C^{18}O^{16}O$ discrimination was crudely estimated using an inversion approach based on the mass balance of $C^{18}O^{16}O$. The mean discrimination value was 10.5‰ (±8.8‰) and was in broad agreement with other canopy scale estimates for C_3 species. The large difference between the isotope signature of respiration and midday canopy photosynthesis (isotopic disequilibrium of ∼20‰) could be very useful for precise partitioning of the net ecosystem CO_2 exchange into photosynthesis and respiration (Ogée et al., 2004).

Acknowledgements

We express our sincere thanks to Bill Breiter (USDA-ARS Biological Field Technician) for his assistance in the field and laboratory. Undergraduate research assistant Ray Anderson was supported with an Undergraduate Research Opportunity fellowship by the College of Agricultural, Food, and Environmental Sciences (COAFES) at the University of Minnesota. Kurt Spokas provided invaluable advice with interfacing the Daqbook and DASYLab software. Iyabo Lawal helped design the flask sampling system and analyzed the flask samples. Mike Dolan (USDA-ARS Technician) provided technical expertise maintaining the isotope ratio mass spectrometer. Dr. Kaycie Billmark and Jianmin Zhang provided comments on an earlier draft of the manuscript. The authors gratefully acknowledge the NOAA Air Resources Laboratory (ARL) for the provision of the HYSPLIT transport and dispersion model website (http://www.arl.noaa.gov/ready.html) used in this manuscript. Financial assistance for this project was provided by a Faculty Development Grant from COAFES (TJG) and was supported by the Office of Science (BER), U.S. Department of Energy, Grant No. DE-FG02-03ER63684 (TJG and JMB) and the U.S. National Science Foundation, Grant No. EAR-0229343 (XL). Finally, we thank Dr. D.R. Bowling and the anonymous reviewers of this manuscript for their helpful comments and criticisms.

References

Allison, C.A., Francey, R.J., Meijer, H.A.J., 1995. Recommendations for the reporting of stable isotope measurements of carbon and oxygen in CO_2 gas. Reference and intercomparison materials for stable isotopes of light elements. IAEA-TECDOC 825, 155–162.

Amundson, R., Stern, L., Baisden, T., Wang, Y., 1998. The isotope composition of soil and soil-respired CO_2. Geoderma 82, 83–114.

Baker, J.M., Griffis, T.J., 2005. Examining strategies to improve the carbon balance of corn/soybean agriculture using eddy covariance and mass balance techniques. Agric. For. Meteorol. 128 (3/4), 163–177.

Blanken, P.D., Black, T.A., Neumann, H.H., den Hartog, G., Yang, P.C., Nesic, Z., Lee, X., 2001. The seasonal water and energy exchange above and within a boreal aspen forest. J. Hydrol. 245, 118–136.

Bowling, D.R., Baldocchi, D.D., Monson, R.K., 1999. Dynamics of isotopic exchange of carbon dioxide in a Tennessee deciduous forest. Glob. Biogeochem. Cycles 13 (4), 903–922.

Bowling, D.R., Tans, P.P., Monson, R.K., 2001. Partitioning net ecosystem CO_2 exchange with isotopic fluxes of CO_2. Global Change Biol. 7, 127–145.

Bowling, D.R., McDowell, N.G., Welker, J.M., Bond, B.J., Law, B.E., Ehleringer, J.R., 2003a. Oxygen isotope content of CO_2 in nocturnal ecosystem respiration. 2. Short-term dynamics of foliar and soil component fluxes in an old-growth ponderosa pine forest. Glob. Biogeochem. Cycles 17 (4), 1124 doi 10.1029/2003GB002082.

Bowling, D.R., McDowell, N.G., Welker, J.M., Bond, B.J., Law, B.E., Ehleringer, J.R., 2003b. Oxygen isotope content of CO_2 in nocturnal ecosystem respiration. 1. Observations in forests along a precipitation transect in Oregon, USA. Glob. Biogeochem. Cycles 17 (4), 1120 doi 10.1029/2003GB002081.

Bowling, D.R., Sargent, S.D., Tanner, B.D., Ehleringer, J.R., 2003c. Tunable diode laser absorption spectroscopy for stable isotope studies of ecosystem–atmosphere CO_2 exchange. Agric. For. Meteorol. 118 (1/2), 1–19.

Bowling, D.R., Burns, S.P., Conway, T.J., Monson, R.K., White, J.W.C., 2005. Extensive observations of CO_2 carbon isotope content in and above a high-elevation subalpine forest. Global Biogeochem. Cycles 19 (3) (Art. No. GB3023).

Cernusak, L.A., Farquhar, G.D., Wong, S.C., Stuart-Williams, H., 2004. Measurement and interpretation of the oxygen isotope composition of carbon dioxide respired by leaves in the dark. Plant Physiol. 136, 3350–3363.

Cernusak, L.A., Farquhar, G.D., Pate, J.S., 2005. Environmental and physiological controls over oxygen and carbon isotope composition of Tasmanian blue gum, Eucalyptus globules. Tree Physiol. 25, 129–146.

Ciais, P., Denning, A.S., Tans, P.P., Berry, J., Randall, D.A., Collatz, G.J., Sellers, P.J., White, J.W.C., Trolier, M., Meijer, H.A.J., Francey, R.J., Monfray, P., Heimann, M., 1997. A three dimensional synthesis study of $\delta^{18}O$ in atmospheric CO_2. I. Surface fluxes. J. Geophys. Res.-Atmos. 102 (D5), 5857–5872.

Cuntz, M., Ciais, P., Hoffmann, G., Knorr, W., 2003a. A comprehensive global three-dimensional model of delta O-18 in atmospheric CO_2. 1. Validation of surface processes. J. Geophys. Res.-Atmos. 108 (D17), 4527 doi 10.1029/2002JD003153.

Cuntz, M., Ciais, P., Hoffmann, G., Allison, C.E., Francey, R.J., Knorr, W., Tans, P.P., White, J.W.C., Levin, I., 2003b. A comprehensive global three-dimensional model of delta O-18 in atmospheric CO_2. 2. Mapping the atmospheric signal. J. Geophys. Res.-Atmos. 108 (D17), 4528 doi 10.1029/2002JD003154.

De Bièvre, P., Gallet, M., Holden, N.E., Barnes, I.L., 1984. Isotopic abundances and atomic weights of the elements. J. Phys. Chem. Ref. Data 13, 809–891.

Draxler, R.R., Rolph, G.D., 2003. HYSPLIT (HYbrid Single-Particle Lagrangian Integrated Trajectory) Model access via NOAA ARL READY Website (http://www.arl.noaa.gov/ready/hysplit4.html). NOAA Air Resources Laboratory, Silver Spring, MD.

Farquhar, G.D., Ehleringer, J.R., Hubick, K.T., 1989. Carbon isotope discrimination and photosynthesis. Ann. Rev. Physiol. Plant Mol. Biol. 40, 503–537.

Farquhar, G.D., Lloyd, J., Taylor, J.A., Flanagan, L.B., Syvertsen, J.P., Hubick, K.T., Wong, S.C., Ehleringer, J.R., 1993. Vegetation effects on the isotope composition of oxygen in atmospheric CO_2. Nature 363, 439–443.

Flanagan, L.B., Brooks, J.R., Varney, G.T., Ehleringer, J.R., 1997. Discrimination against $C^{18}O^{16}O$ during photosynthesis and the oxygen isotope ratio of respired CO_2 in boreal forest ecosystems. Glob. Biogeochem. Cycles 11, 83–98.

Flanagan, L.B., Ehleringer, J.R., 1998. Ecosystem–atmosphere CO_2 exchange: interpreting signals of change using stable isotope ratios. Trends Ecol. Evol. 13 (1), 10–14.

Flanagan, L.B., Kubien, D.S., Ehleringer, J.R., 1999. Spatial and temporal variation in the carbon and oxygen stable isotope ratio of respired CO_2 in a boreal forest ecosystem. Tellus Series B: Chem. Phys. Meteorol. 51 (2), 367–384.

Francey, R.J., Tans, P.P., 1987. Latitudinal variation in oxygen-18 of atmospheric CO_2. Nature 327, 495–497.

Fung, I., Field, C.B., Berry, J.A., Thompson, M.V., Randerson, J.T., Malmstrom, C.M., Vitousek, P.M., Collatz, G.J., Sellers, P.J., Randall, D.A., Denning, A.S., Badeck, F., John, J., 1997. Carbon 13 exchanges between the atmosphere and biosphere. Glob. Biogeochem. Cycles 11 (4), 507–533.

Gemery, P.A., Trolier, M., White, J.W.C., 1996. Oxygen isotope exchange between carbon dioxide and water following atmospheric sampling using glass flasks. J. Geophys. Res.-Atmos. 101, 14415–14420.

Gillon, J., Yakir, D., 2001. Influence of carbonic anhydrase activity in terrestrial vegetation on the O-18 content of atmospheric CO_2. Science 291 (5513), 2584–2587.

Griffis, T.J., Baker, J.M., Sargent, S., Tanner, B.D., Zhang, J., 2004. Measuring field-scale isotopic CO_2 fluxes using tunable diode laser absorption spectroscopy and micrometeorological techniques. Agric. For. Meteorol. 124, 15–29.

Griffis, T.J., Baker, J.M., Zhang, J., 2005. Seasonal dynamics of isotopic CO_2 exchange in a C_3/C_4 managed ecosystem. Agric. For. Meteorol. 132, 1–19.

Helliker, B.R., Roden, J.S., Cook, C., Ehleringer, J.R., 2002. A rapid and precise method for sampling and determining the oxygen isotope ratio of atmospheric water vapor. Rapid Commun. Mass Spectrom. 16, 929–932.

Hesterburg, R., Siegenthaler, U., 1991. Production and stable isotopic composition of CO_2 in soil near Bern Switzerland. Tellus Series B: Chem. Phys. Meteorol. 43, 197–205.

Ishizawa, M., Nakazawa, T., Higuchi, K., 2002. A multi-box model study of the role of the biospheric metabolism in the recent decline of $\delta^{18}O$ in atmospheric CO_2. Tellus Series B: Chem. Phys. Meteorol. 54, 307–324.

Kato, T., Nakazawa, T., Aoki, S., Sugawara, S., Ishizawa, M., 2004. Seasonal variation of the oxygen isotopic ratio of atmospheric carbon dioxide in a temperate forest, Japan. Glob. Biogeochem. Cycles 18 (2) (Art. No. GB2020).

Keeling, C.D., 1958. The concentration and isotopic abundances of atmospheric carbon dioxide in rural areas. Geochim. Cosmochim. Acta 13, 322–334.

Kroopnick, P., Craig, H., 1972. Atmospheric oxygen: isotopic composition and solubility fractionation. Science 175, 54–55.

Lai, C.T., Schauer, A.J., Owensby, C., Ham, J.M., Ehleringer, J.R., 2003. Isotopic air sampling in a tallgrass prairie to partition net ecosystem CO_2 exchange. J. Geophys. Res.-Atmos. 108 (D18) doi 10.1029/2002JD003369 (Art. No. 4566).

Lee, X., Bullock, O.R., Andres, R.J., 1991. Anthropogenic emission of mercury to the atmosphere in the northeast United States. Geophys. Res. Lett. 28 (7), 1231–1234.

Lee, X., Sargent, S., Smith, R., Tanner, B., 2005. In-situ measurement of water vapor isotopes for atmospheric and ecological applications. J. Atmos. Oceanic Technol. 22, 555–565.

Lloyd, J., Kruijt, B., Hollinger, D.Y., Grace, J., Francey, R.J., Wong, S.C., Kelliher, F.M., Miranda, A.C., Farquhar, G.D., Gash, J.H.C., Vygodskaya, N.N., Wright, I.R., Miranda, H.S., Schulze, E.D., 1996. Vegetation effects on the isotopic composition of atmospheric CO_2 at local and regional scales: theoretical aspects and a comparison between rain forest in Amazonia and a boreal forest in Siberia. Aust. J. Plant Physiol. 23 (3), 371–399.

Lloyd, J., Langenfelds, R.L., Francey, R.J., Gloor, M., Tchebakova, N.M., Zolotoukhine, D., Brand, W.A., Werner, R.A., Jordan, A., Allison, C.A., Zrazhewske, V., Shibistova, O., Schulze, E.D., 2002. A trace-gas climatology above Zotino, central Siberia. Tellus Series B: Chem. Phys. Meteorol. 54 (5), 749–767.

Miller, J.B., Yakir, D., White, J.W.C., Tans, P.P., 1999. Measurement of O-18/O-16 in the soil–atmosphere CO_2 flux. Glob. Biogeochem. Cycles 13, 761–774.

Monin, A.S., Obukhov, A.M., 1954. Basic laws of turbulent mixing in the atmospheric surface layer. Trans. Geophys. Inst. Akad. Nauk. USSR 24 (151), 163–187.

Mortazavi, B., Chanton, J.P., 2002. Carbon isotopic discrimination and control of nighttime canopy delta O-18–CO_2 in a pine forest in the southeastern United States. Glob. Biogeochem. Cycles 16 (1) (Art. No. 1008).

Ogée, J., Peylin, P., Ciais, P., Bariac, T., Brunet, Y., Berbigier, P., Roche, C., Righcard, P., Bardoux, G., Bonnefond, J.M., 2003. Partitioning net ecosystem carbon exchange into net assimilation

and respiration using (CO_2)–C-13 measurements: a cost-effective sampling strategy. Glob. Biogeochem. Cycles 17 (2), 1070 doi 10.1029/2002GB001995.

Ogée, J., Peylin, P., Cuntz, M., Bariac, T., Brunet, Y., Berbigier, P., Richard, C., Ciais, P., 2004. Partitioning net ecosystem carbon exchange into net assimilation and respiration with canopy-scale isotopic measurements: an error propagation analysis with $^{13}CO_2$ and $CO^{18}O$ data. Glob. Biogeochem. Cycles 18 (2), GB2019 doi 10.1029/2003GB002166.

Pataki, D.E., Ehleringer, J.R., Flanagan, L.B., Yakir, D., Bowling, D.R., Still, C.J., Buchmann, N., Kaplan, J.O., Berry, J.A., 2003a. The application and interpretation of Keeling plots in terrestrial carbon cycle research. Glob. Biogeochem. Cycles 17 (1), 1022 doi 10.1029/2001GB001850.

Pataki, D.E., Bowling, D.R., Ehleringer, J.R., 2003b. Seasonal cycle of carbon dioxide and its isotopic composition in an urban atmosphere: anthropogenic and biogenic effects. J. Geophys. Res.-Atmos. 108 (D23), 4735 doi 10.1029/2003JD003865.

Raupach, M.R., 1989. A practical Lagrangian method for relating scalar concentrations to vegetation canopies. Quart. J. Roy. Meteorol. Soc. 115, 609–632.

Riley, W.J., Still, C.J., Torn, M.S., Berry, J.A., 2002. A mechanistic model of (H_2O)–O-18 and (COO)–O-18 fluxes between ecosystems and the atmosphere: model description and sensitivity analyses. Glob. Biogeochem. Cycles 16 (4) (Art. No. 1095).

Riley, W.J., Still, C.J., Helliker, B.R., Ribas-Carbo, M., Berry, J.A., 2003. O-18 composition of CO_2 and H_2O ecosystem pools and fluxes in a tallgrass prairie: simulations and comparisons to measurements. Global Change Biol. 9 (11), 1567–1581.

Schuepp, P.H., Leclerc, M.Y., MacPherson, J.I., Desjardins, R.L., 1990. Footprint predictions of scalar fluxes from analytical solutions of the diffusion equation. Boundary-Layer Meteorol. 50, 355–373.

Simpson, I.J., Thurtell, G.W., Neumann, H.H., den Hartog, G., Edwards, G.C., 1998. The validity of similarity theory in the roughness sublayer above forests. Boundary-Layer Meteorol. 87, 69–99.

Sternberg, L.da.S.L., Moreira, M.Z., Martinelli, L.A., Victoria, R.L., Barbosa, E.M., Bonates, C.M., Nepstad, D., 1998. The relationship between 18O/16O and 13C/12C ratios of ambient CO_2 in two Amazonian tropical forests. Tellus Series B: Chem. Phys. Meteorol. 50, 366–376.

Styles, J.M., Lloyd, J., Zolotoukhine, D., Lawton, K.A., Tchebakova, N., Francey, R.J., Arneth, A., Salamakho, D., Kolle, O., Schulze, E.D., 2002. Estimates of regional surface carbon dioxide exchange and carbon and oxygen isotope discrimination during photosynthesis from concentration profiles in the atmospheric boundary layer. Tellus Series B: Chem. Phys. Meteorol. 54 (5), 768–783.

Tans, P.P., Berry, J.A., Keeling, R.F., 1993. Oceanic $^{13}C/^{12}C$ observation: a new window on ocean CO_2 uptake. Glob. Biogeochem. Cycles 7, 353–368.

Tans, P.P., 1998. Oxygen isotopic equilibrium between carbon dioxide and water in soils. Tellus Series B: Chem. Phys. Meteorol. 50, 163–178 (Correction, Tellus Series B, 50, 400, 1998).

Trolier, M., White, J.W.C., Tans, P.P., Masarie, K.A., Gemery, P.A., 1996. Monitoring the isotopic composition of atmospheric CO_2: measurements from the NOAA global air sampling network. J. Geophys. Res.-Atmos. 101 (D20), 25897–25916.

Verkouteren, R.M., Lee, J.N., 2001. Web-based interactive data processing: application to stable isotope metrology. Fresenius J. Anal. Chem. 370, 803–810.

Wang, X.F., Yakir, D., Avishai, M., 1998. Non-climatic variations in the oxygen isotopic compositions of plants. Global Change Biol. 4 (8), 835–849.

Yakir, D., Sternberg, L.D.L., 2000. The use of stable isotopes to study ecosystem gas exchange. Oecologia 123 (3), 297–311.

Yakir, D., Wang, X.F., 1996. Fluxes of CO_2 and water fluxes between terrestrial vegetation and the atmosphere estimated from isotope measurements. Nature 380, 515–517.

Zhang, J., Griffis, T.J., Baker, J.M., 2005. Using continuous stable isotope measurements to partition net ecosystem CO_2 exchange. Plant Cell Environ., doi:10.1111/j.1365-3040.2005.01425.x.